Acta Oceanol. Sin., 2017, Vol. 36, No. 7, P. 4–14
DOI: 10.1007/s13131-017-1078-z
http://www.hyxb.org.cn
E-mail: hyxbe@263.net

Pacific-Indian interocean circulation of the Antarctic Intermediate Water around South Australia

YAO Wenjun[1]*, SHI Jiuxin[1]

[1] Key Laboratory of Physical Oceanography, Ocean University of China, Qingdao 266100, China

Received 31 December 2016; accepted 8 February 2017

Abstract

On the basis of the salinity distribution of isopycnal (σ_0=27.2 kg/m^3) surface and in salinity minimum, the Antarctic Intermediate Water (AAIW) around South Australia can be classified into five types corresponding to five regions by using *in situ* CTD observations. Type 1 is the Tasman AAIW, which has consistent hydrographic properties in the South Coral Sea and the North Tasman Sea. Type 2 is the Southern Ocean (SO) AAIW, parallel to and extending from the Subantarctic Front with the freshest and coldest AAIW in the study area. Type 3 is a transition between Type 1 and Type 2. The AAIW transforms from fresh to saline with the latitude declining (equatorward). Type 4, the South Australia AAIW, has relatively uniform AAIW properties due to the semi-enclosed South Australia Basin. Type 5, the Southeast Indian AAIW, progressively becomes more saline through mixing with the subtropical Indian intermediate water from south to north. In addition to the above hydrographic analysis of AAIW, the newest trajectories of Argo (Array for real-time Geostrophic Oceanography) floats were used to constructed the intermediate (1 000 m water depth) current field, which show the major interocean circulation of AAIW in the study area. Finally, a refined schematic of intermediate circulation shows that several currents get together to complete the connection between the Pacific Ocean and the Indian Ocean. They include the South Equatorial Current and the East Australia Current in the Southwest Pacific Ocean, the Tasman Leakage and the Flinders Current in the South Australia Basin, and the extension of Flinders Current in the southeast Indian Ocean.

Key words: Antarctic Intermediate Water, Pacific-Indian interocean circulation, South Australia, World Ocean Circulation Experiment, Argo

Citation: Yao Wenjun, Shi Jiuxin. 2017. Pacific-Indian interocean circulation of the Antarctic Intermediate Water around South Australia. Acta Oceanologica Sinica, 36(7): 4–14, doi: 10.1007/s13131-017-1078-z

1 Introduction

The Antarctic Intermediate Water (AAIW) is characterized by vertical salinity minimum, extends just north of Subantarctic Front (SAF) (Orsi et al., 1995) and lies in 600–1 200 m depth water layers, with potential density (σ_0) ranging between 27.1 and 27.3 kg/m^3 (Piola and Georgi, 1982). The identification of AAIW can be traced through the subtropical gyres around the Southern Ocean (SO) and father north into the Northern Hemisphere (Talley, 1996).

AAIW plays important roles in the global ocean circulation, such as: (1) it ventilates the lower thermocline water in the subtropical gyres (Sloyan and Rintoul, 2001); (2) it is the northern limb of Southern Hemisphere super gyre (Speich et al., 2002; Ridgway and Dunn, 2007); (3) it is the return branch of Meridional Overturning Circulation in the Atlantic Ocean (Donners and Drijfhout, 2004; Speich et al., 2007; Talley, 2013).

The traditional way to explore the large-scale circulation of AAIW is to trace the geophysical and geochemical properties of water mass, such as salinity, temperature, potential vorticity, and oxygen, along certain isopycnal surface within the AAIW layers (Reid, 1989; Talley, 1996; McCarthy and Talley, 1999). However, since the 21st century, the circulation of AAIW in the Southern Hemisphere becomes increasingly accurate and distinct. This is due to the conduction of autonomous floats as part of the World Ocean Circulation Experiment (WOCE) program (Davis et al., 2001), and the expanded trajectories of Argo (Array for Real-time Geostrophic Oceanography) floats (Park et al., 2005; Lebedev et al., 2007). Using the autonomous floats, Davis (2005) has depicted the overview circulation of intermediate water in the Pacific and Indian Oceans, and through the analysis of Argo float trajectories, Bostock et al. (2013) has reviewed the circulation of AAIW in the South Pacific Ocean.

Many works have been conducted to research the AAIW circulation in the individual ocean basin around Australia by using the temperature and salinity observations (Schodlok and Tomczak, 1997; Sokolov and Rintoul, 2000; Ridgway and Dunn, 2003; Wong, 2005). However, it is still necessary to overview the AAIW circulation connecting the Pacific Ocean and the Indian Ocean, especially the south of Australia, which is the key region for water mass exchange between the Pacific Ocean and the Indian Ocean apart from the Antarctic Circumpolar Current (ACC), but it was paid relatively less attention historically.

This work is to study the Pacific-Indian interocean circulation of the AAIW. We first separated the AAIW into different types, based on their different potential temperature (θ) and salinity (S) values of the isopycnal surface and in the salinity minimum. Further we constructed the climatological current field in the AAIW layer (at 1 000 m water depth), to compare with the

Foundation item: The Chinese Polar Environment Comprehensive Investigation and Assessment Programs under contract Nos CHINARE-04-04 and CHINARE-04-01.
*Corresponding author, E-mail: wjimyao@gmail.com

previous conclusions of AAIW circulation in the study area. At the end of this paper, a refined schematic of AAIW circulation was conducted.

2 Data and methods

There are eight sections from the WOCE program used in this study. Their locations are denoted in Fig. 1 and information listed in Table 1 (refer to http://cchdo.ucsd.edu/). In order to avoid introducing decadal variations of the hydrographic properties due to the time interval of measurements, the sections used here were quasi-synchronous, observed between April 1993 and May 1996.

Table 1. WOCE voyages in the oceans connecting the south Pacific and Indian Oceans

Voyage No.	Time	Ship	Country	Chief scientist
P11A	Apr.–May 1993	*Aurora Australis*	Australia	Rintoul Stephen R.
P11S	Jun.–Jul. 1993	*Franklin*	Australia	Church John A.
PR11/PR13N	Sep.–Oct. 1993	*Franklin*	Australia	Church John A.
S05	Nov.–Dec. 1994	*Franklin*	Australia	Tomczak Matthias
I08S/I09S	Dec. 1994–Jan. 1995	*Knorr*	USA	McCartney Mike
SR03	Jan.–Feb. 1995	*Aurora Australis*	Australia	Rintoul Stephen R.
I05	Mar.–Apr. 1995	*Knorr*	USA	Talley Lynne
ISS3	May 1996	*Franklin*	Australia	McDougall Trevor J.

The objectively analyzed climatological fields of temperature and salinity are from World Ocean Atlas 2013 (WOA13) Version 2. They are derived from the *in situ* temperature and salinity observed from 2005 to 2012, when the temperature and salinity profiles have tremendously expanded attributable to the development of Argo program (Roemmich et al., 2015). Due to its greatly increased samplings, it is believable that the WOA13 data around Australia are more accurate than those used in the previous studies (Dunn and Ridgway, 2002; Ridgway and Dunn, 2003).

The Argo floats are designed to take approximately 10 d to complete a typical cycle. The float first descends to the subsurface at a certain depth (always around 1 000 m). They drift for 9 d before ascending to the sea surface over another 8 h. This work pattern makes it available to determine the intermediate current velocity. The YoMaHa'07 data, derived from the trajectories of Argo floats at the parking level (1 000 m), provides the individual estimates of velocities of subsurface currents and their error estimates (http://apdrc.soest.hawaii.edu/projects/yomaha/index.php) (Lebedev et al., 2007). The estimated velocities in the region for the Pacific-Indian interocean circulation (25°–53°S, 100°–165°E) were used here.

In addition, several criteria were applied to screen the velocity data. Only those Argo floats with velocity components (both meridional and zonal) less than 0.5 m/s and parking pressure centered on 1 000 m were selected. Eventually, a total number of 44 967 velocity vector over the period from August 2001 to August 2015 were collected, with 24.3%, 25.4%, 25.8% and 24.5% of them for the austral spring (October–December), summer (January–March), autumn (April–June) and winter (July–September), respectively. The error sources for the derived velocity, including position measurement, clock drift and unknown drift during ascending and descending phases, give rise to a measurement error of 8×10^{-3} m/s (Bostock et al., 2013). In order to construct a climatological field of deep currents, the discrete velocity vector from the Argo floats were interpolated onto a fine resolution of (1/2)°×(1/2)° with Kriging interpolation method. Note that here the variogram of Kriging gridding method is linear and with no nugget effect.

Apparent oxygen utilization (AOU) is the difference between equilibrium saturated and dissolved concentration under the same physical and chemical situation (Garcia et al., 2006). Usually, it is used to study the age of the water mass, with high value relating to old age (McCarthy et al., 2011). Compared with the dissolved oxygen, which could also be proxy for water mass age, the AOU is more favorable because it considers the effect of water temperature. In this study, the AOU on a certain isopycnal would be plotted against the salinity to reflect the relationship between the hydrological properties of AAIW and its ventilation.

3 AAIW distribution around South Australia

The area of interest is shown in Fig. 1, which consists of the Southwest Pacific Ocean, the South Australia Basin and the Southeast Indian Ocean. In the following subsections, the potential temperature versus salinity (θ-S, hereafter potential temperature is referred to potential temperature referenced to the sea surface unless otherwise state) diagrams of the representative stations are shown to distinguish the AAIW between the Pacific Ocean and the Indian Ocean. And then the mixing, transporting and transitioning processes of the AAIW are displayed. In this work, we focus on the AAIW layers with the potential density (σ_0) ranging between 27.0 kg/m^3 and 27.5 kg/m^3 (Figs 2 and 3).

As described in the introduction, AAIW is identified as a characteristic of a salinity minimum in intermediate water depth. AAIW in different ocean basins around the South Australia has distinct properties as shown in Fig. 2 and Table 2. Those in the Southwest Pacific (SWP) are the most saline ones. Meanwhile those in the SO are the freshest ones. The θ-S curves of AAIW in the Southeast Indian (SEI) and the South Australia Basin are quite similar in the upper layer, but in the deeper layer the cluster of SEI displays a more saline characteristic. Following the above overview, we further discussed the property distribution of AAIW region by region.

3.1 *Water mass distribution southeast of Australia*

In the Southwest Pacific Ocean, there are vigorous mixing and intense exchange between the salty (warm) AAIW of subtropical Pacific Ocean and the fresh (cold) one of SO. In the south Coral Sea and the North Tasman Sea, the AAIW is quite consistent with its minimum salinity ranging between 34.45 and 34.46 (Fig. 3d, Stas 1–6, note that the station nomenclatures are independent among Figs 3d–f). This is the most saline AAIW in the region of interest, due to the feeding of salty (warm) AAIW from the east carried by the South Equatorial Current (SEC) and then the East Australia Current (EAC). More detailed, the minimum salinity at Sta. 1 (≈27°S) decreases by 0.01 comparing with Sta. 2 (≈30°S) in just 3° further south. But the minimum salinity at Stas 2–6 differs only 0.005 from each other in a 13° latitude band. This AAIW truncation between Sta.1 and Stas 2–6 is presumably

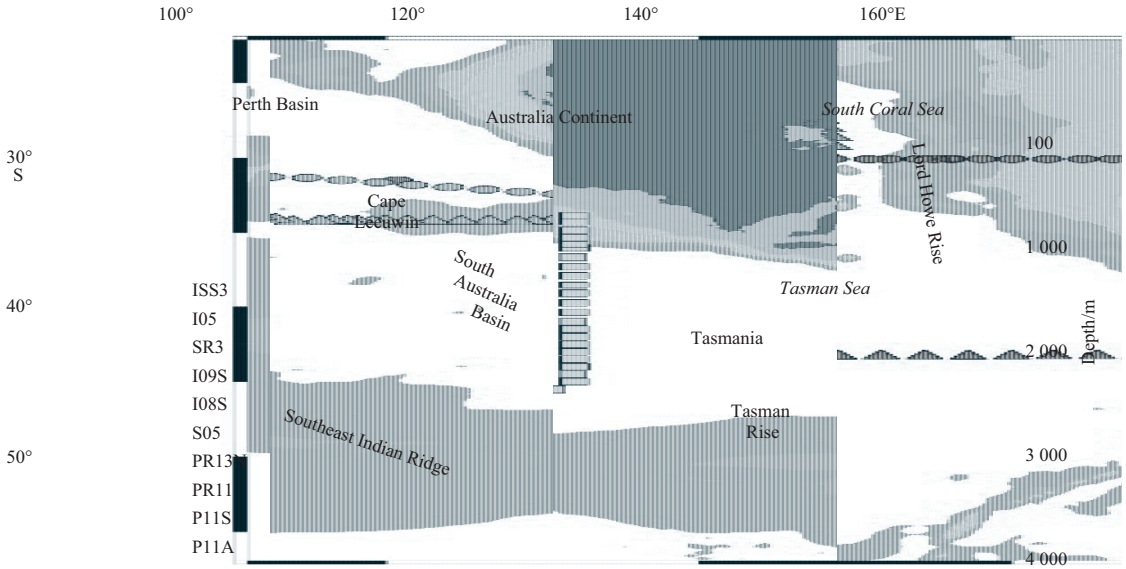

Fig. 1. Bathymetry and WOCE CTD sections around South Australia with main bathymetric features labelled. Stations of CTD are ticked by different markers with their voyage numbers listed at the left bottom.

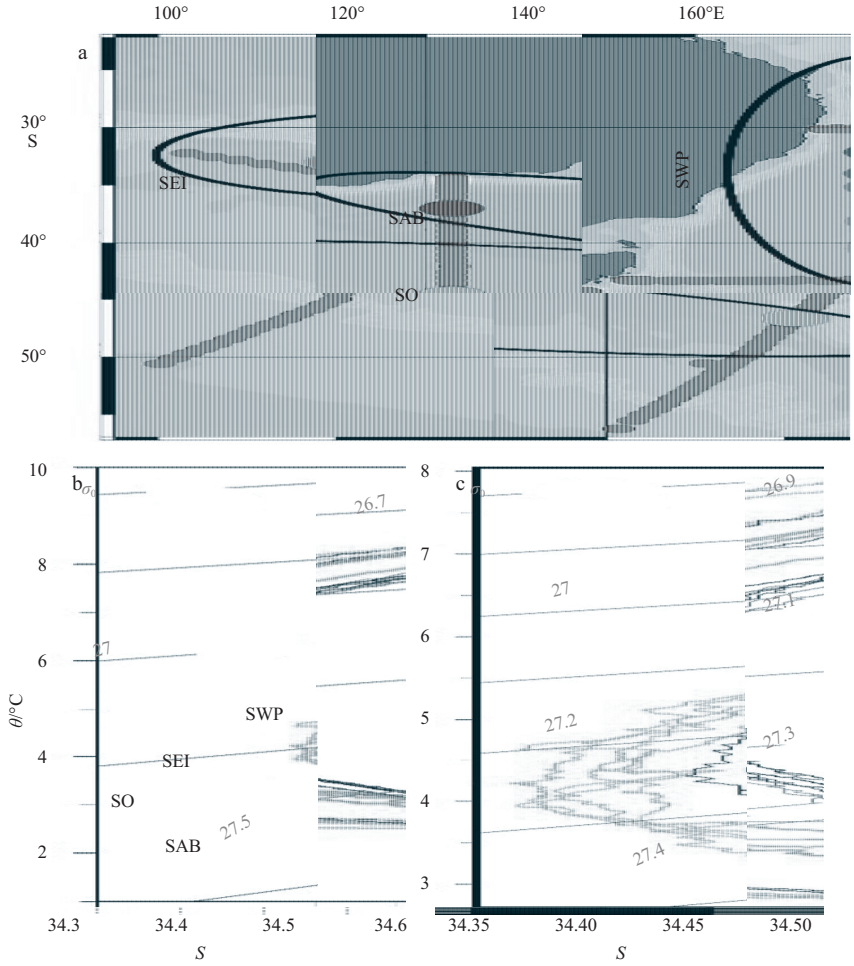

Fig. 2. The stations (a) and the θ-S curves (b) for clusters in SWP (Southwest Pacific), SEI (Southeast Indian), SO (Southern Ocean) and SAB (South Australia Basin), (c) is the magnification of (b), in the core layer of AAIW.

caused by an inflow of subtropical salty (warm) intermediate water, which enters the south Coral Sea at 28°S directly from the east (Sokolov and Rintoul, 2000).

The Tasman Front (TF), approximately located at 35°S (Ridg-

Table 2. The values of the salinity in the salinity minimum used to identify the different AAIW described in Section 3.

Area	*S*
SWP (Southwest Pacific)	34.44–34.46
SEI (Southeast Indian)	34.38–34.39
SO (Southern Ocean)	34.34–34.36
SAB (South Australia Basin)	34.37–34.38

way and Dunn, 2003; Hamilton, 2006), forms a zonal physical barrier of the water mass properties. Comparing the θ-S curves of Stas 6–7, it clearly shows that the minimum salinity of AAIW rapidly reduces by 0.03 from north to south. Such a phenomenon reveals the obstruction effect of the TF, preventing the salty AAIW in the north entering into the South Tasman Sea.

Apart from the replenishment coming from north, the AAIW in the Tasman Sea is also fed by the SO AAIW form the south. Earliest work found that no fresh AAIW from the south spreads further to the north than the latitude of STF (Subtropical Front) (Wyrtki, 1962). But later, Tomczak and Godfrey (1994) observed the spreading as north to 28°S. More recently, by using a θ-S curve approach, Hamilton (2006) revealed that the fresh AAIW from the south does propagate into the Tasman Sea. Due to the formation mechanism by subsurface mixing across the SAF (Molinelli, 1981), the AAIW at Sta. 11 is largely characterized by the features of SO AAIW (fresh and cold). Away from the most ventilated AAIW just north of the SAF, such fresh and cold features rapidly fade away (Sta. 8).

From Fig. 3d, the AAIW in the Tasman Sea (curve at Sta. 9) has the same properties with that observed in the South Coral Sea (curves at Stas 1–6), suggesting that the AAIW in the West Tasman Sea is carried by the EAC. Further southwest, just south of Tasmania and north of 46°S, θ-S curve at Sta. 10 also overlays the envelop of curves at Stas 1–6 and 9, except that the AAIW at Sta. 10 is fresher and colder in the lower layers (≈27.25–27.5 σ_0). So it would be safe to state that the EAC carries the AAIW from the Coral Sea to the Tasman Sea. And this water mass further flows southwestward to the south of Tasmania across the SR3 section (Rintoul and Sokolov, 2001), which is the Tasman Leakage (TL) or Tasman Outflow (TO) (Rintoul and Sokolov, 2001; Rosell-Fieschi et al., 2013).

3.2 *Water mass distribution south of Australia*

In order to compare with the water mass properties in the Southwest Pacific Ocean, Stas 10–11 in Fig. 3d are still retained in Fig. 3e, as shown by the same color dots/curves (the nomenclatures are reallocated in Fig. 3e). In the ocean south of Australia, the selected CTD stations can be divided into three groups based on their different θ-S properties.

The AAIW south of Tasmania and north of 46°S in the SR3 section comes from the Tasman Sea. As shown by the θ-S curves in Fig. 3e, the AAIW at Sta. 1 is quite different from the other AAIW in the present region with distinctly higher salinity (Fig. 3b). It is a pity that there is no sufficient CTD measurements between the SR3 section and the eastern branch of S05 section. Therefore, it could not trace the flowing process of this AAIW further west. But a little effort is made to fill this data gap in the below sections to reveal its propagation through the South Australia Basin, which will be discussed later.

As delineated by Figs 3b and e, the AAIW at Stas 2–6 mainly represents the water mass properties in the South Australia Basin, with a minimum salinity ranging between 34.36 and 34.38. The AAIW in the South Australia Basin is relatively coherent because of the semi-enclosed topography, bounded by the Australia Continent to the north, the Southeast Indian Ridge to the south and the Tasman Rise to the east (Fig. 1). The AAIW at Stas 2–6 is distinctly fresher and colder than that at Sta. 1 (Fig. 3e), implying that the hydrological signal carried by the latter completely vanishes at least at the longitude of S05 section.

The AAIW at Stas 7–9 is characterized by the fresh and cold SO AAIW extending from the SAF, where the AAIW forms through subsurface mixing along isopycnal. Owing to the swing

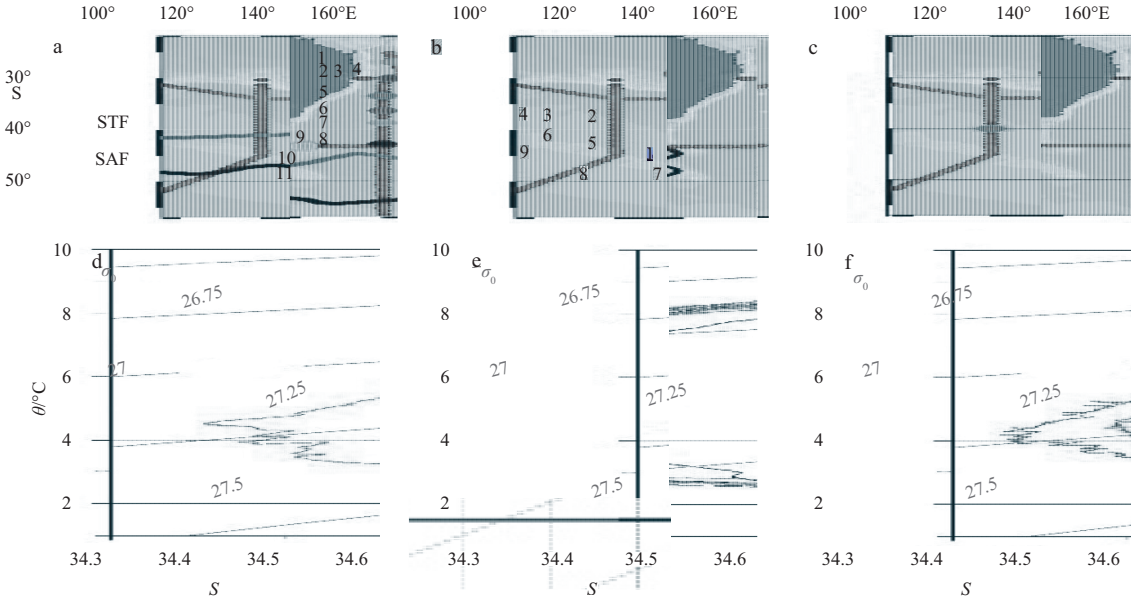

Fig. 3. Selected CTD stations with different colors and their corresponding θ-S curves east of Australia (a, d), south of Australia (b, e) and west of Australia (c, f). Sequential numbers are used for analysis in Section 3.1 (a) and Section 3.2 (b). Gray and black lines in Fig. 3a represent the position of Subtropical Front (STF) and Subantarctic Front (SAF), respectively. Circles in Fig. 3b denote different AAIW described in Section 3.2.

and the meandering of SAF, the θ-S curves of the SO AAIW has more spikes, and the width of envelop is broader than that in the South Australia Basin.

3.3 *Water mass distribution southwest of Australia*

Part of the AAIW in the Southeast Indian Ocean comes from the South Australia Basin and further originates from the Southwest Pacific Ocean (Fine, 1993; Rintoul and Sokolov, 2001; Wong, 2005). Wong (2005) proposed that the smallest meridional gradient of isopycnal salinity in the AAIW layers locates in the latitude band of 30°–40°S and east of 55°E, where the salinity variation of AAIW isopycnal surface is less than 0.08. It implies that this is an ideal region for the study of the decadal variability of AAIW in the South Indian Ocean. Even though there are the smallest salinity gradient suggested by Wong (2005), it is still not quite significant for the consistency of θ-S properties of large-scale AAIW (Fig. 3f).

The AAIW here shows that the salinity increases and temperature rises with latitude declining (equatorward), through mixing with the subtropical Indian intermediate water. Along the western Australian coast and above 1 000 m depth, a temperature range of 4.5–8.0°C at the salinity minimum has been observed (Woo and Pattiaratchi, 2008), which is a larger range of temperature than that in the Perth Basin (PB) (Fig. 3f).

4 Isopycnal properties on 27.2σ_0 surface

Mapping the isopycnal properties is an effective way to explore the large-scale circulation of AAIW, under the assumption that the water mass flows along isopycnal with vertical/lateral mixing being ignored. Reid (1989) and Talley (1996) have illustrated the distribution of isopycnal properties of AAIW in the South Atlantic Ocean and the global ocean, respectively. The typical isopycnal surface of AAIW, σ_0=27.2 kg/m^3, is chosen here. In addition, because the temperature and salinity on the isopycnal surface are compensatory, we only discuss the latter variable.

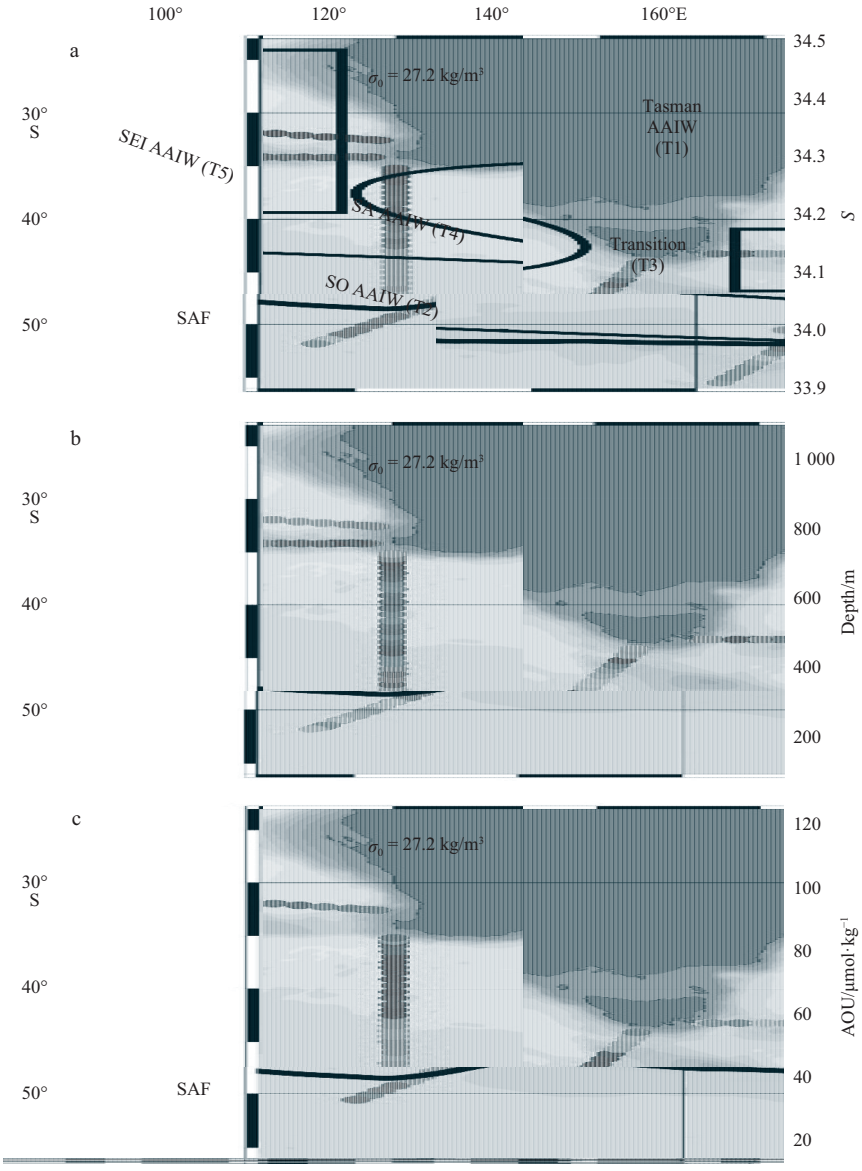

Fig. 4. Salinity on σ_0=27.2 kg/m^3 isopycnal surface (a). Tasman AAIW (Type 1), SO AAIW (Southern Ocean AAIW, Type 2), Transition (Type 3), SA AAIW (South Australia AAIW, Type 4) and SEI AAIW (Southeast Indian AAIW, Type 5) are described in Section 4. The same as Fig. 4a, but for depth and without five areas delineating (b). The same as Fig. 4b, but for AOU (c). The thick black lines in Figs 4a–c represent the position of Subantarctic Front.

The mapping result (Fig. 4a) is similar to that revealed by the θ-S diagram, but shows an overview of the isopycnal salinity of AAIW. According to the distribution of isopycnal salinity values, the AAIW could be classified into five types corresponding to different regions. Note that the 27.2 σ_0 isopycnal south of the SAF has risen to the sea surface and lost the characteristic of salinity minimum, so it can not represent AAIW anymore.

Type 1 is the Tasman AAIW, which is consistent with about 34.45 isopycnal salinity, with variations less than 0.01 in 10° latitude interval. Type 2 is the SO AAIW, characterized by the lowest temperature and salinity, due to the replenishment from the Antarctic Surface Water (AASW) through mixing along isopycnal. Type 3 is the transition between Type 1 and Type 2, the salinity decreases by more than 0.05 in a relatively short distance (700 km). Type 4 is the South Australia AAIW. As a semi-enclosed region, the AAIW in the South Australia Basin seems to be poorly ventilated (with age about 21–24 a on SR3 (Rintoul and Bullister, 1999) north of 50°S, and 18–24 a along 120°E north of 45°S (Fine et al., 2008), but lack of the age estimates in the basin), and has a relative uniform salinity distribution. Type 5 is located in the Southeast Indian Ocean. It has neither barrier to the north like the South Australia Basin nor enclosed abyssal like the South Coral Sea/North Tasman Sea. As shown in Fig. 4a, the isopycnal salinity progressively increases northward as the AAIW core (salinity minimum) experiences (Fig. 3f).

The isopycnal depth distribution (Fig. 4b) is a little different from that of the salinity. The AAIW plunges steeply northward from the SAF, forming a narrow transition band parallel to the SAF. The isopycnal depth reaches a peak in the abyssal region where the bathymetry is larger than 4 000 m (Fig. 1). And then it begins to shoal from greater than 1 100 m to less than 800 m in the Southeast Indian Ocean, and to less than 900 m in the north of South Australia Basin. A similar northward shoaling in the ocean west of Australia was described by Fieux et al. (2005), which shows that the AAIW core (around 27.2 σ_0) ascends northward from 1 000 to 800 m. There is an asymmetry between the oceans west and east of Australia in Fig. 4b. Along the P11A/S sections at approximately 155°E, the isopycnal depth in the South Coral Sea again descends to greater than 1 000 m after it being at 1 000 m in the North Tasman Sea.

Figure 4c is the AOU of 27.2 σ_0 isopycnal, which shows a quite similar pattern to that of the salinity. Thus the discussion here focuses on their relationship, by displaying the scatter plot of the AOU against the salinity (both of 27.2 σ_0 isopycnal). Although the oxygen data in the ISS3 and the P11A sections are missing, it would not affect the discussion and conclusions below. The correlation coefficient between the AOU and the salinity is 0.97 (Fig. 5), indicating that high salinity corresponds to high AOU as well as old water mass. This is a result of AAIW formation and transport processes. The formation theories of the AAIW include that it ventilates in the local Southeast Pacific Ocean and circumpolarly in the Subantarctic Zone north of the SAF. Both of these theories indicate that the newest AAIW is freshest, coldest and with the lowest AOU (highest dissolved oxygen). When it spreads into subtropical oceans, the most ventilated one is eroded through mixing with surrounding waters, inducing more saline and high AOU (consuming oxygen) AAIW.

5 AAIW circulation in the South Australia Basin from sequential meridional sections of geostrophic velocity

TL is the extension of EAC along the eastern Australian coast, which turns west at south of Tasmania. It shares the same θ-S characteristics of the Coral Sea and the west Tasman Sea AAIW

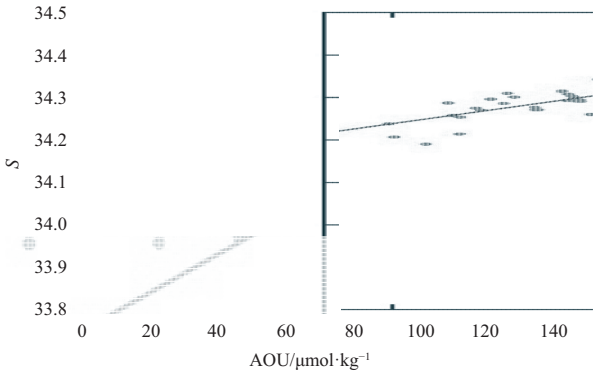

Fig. 5. Scatter plot (blue dots) of the AOU against the salinity (both of σ_0=27.2 kg/m^3 isopycnal) with the red line denoting the linear regression line. Correlation coefficient between the salinity and the AOU is calculated as 0.97. Values are derived from CTD measurements shown in Fig. 1 but without the ISS3 and the P11A sections because of oxygen data missing.

(Rintoul and Bullister, 1999; Ridgway and Dunn, 2007). Combining the work of Fine (1993), Talley (1996) and You (1998), a northwestward flow of the AAIW from south of Australia enters into the subtropical gyre of South Indian Ocean, which is fed by the EAC. Using the data of S05 section (Fig. 1), Schodlok and Tomczak (1997) showed that the AAIW between 120°E and 132°E flows westward at north of the SAF. However, it is still necessary to reveal the complete AAIW circulation in the South Australia Basin, especially the propagation of TL signal west of the SR3 section.

Figures 6a–e display the sequential sections of zonal geostrophic velocity, calculated from the WOA13 temperature and salinity fields. Because of what we focus on is the AAIW that centered at approximately 1 000 m depth, the referenced level of no motion chosen here is 2 000 m depth. And no interpolation is applied in slope and shelf regions where the water depth is less than 2 000 m.

In the section along 146°E (Fig. 6a), we can see that a major current at north of the SAF (49°S), dominantly flows westward with a velocity magnitude no larger than 4 cm/s in the intermediate layer (1 000 m depth). The flowing directions north and south of the SAF are opposite. The largest westward velocity of AAIW appears north of 46°S. This is the TL or TO with a volume transport of approximately 3.0×10^6–8.0×10^6 m^3/s, obtained from observations and numerical models (Speich et al., 2002; Weijer et al., 2012; Rosell-Fieschi et al., 2013). On the basis of analysis of hydrographic θ-S diagrams, there is an anticyclonic (anticlockwise) recirculation in the SR3 section, with the eastward limb lying between 50°S and 48°S, and the westward limb between 48°S and 46°S (Rintoul and Sokolov, 2001). This recirculation can also be identified in Fig. 6a, which shows the velocity direction change in the similar latitude band. It is worth noted that a narrow eastward current, sandwiched between the two westward currents, shows a relatively small velocity magnitude and centers at 46.5°S. But the velocity section of 145.6°E (Fig. 6b), just 70 km away to the west of 146°E section, shows that this sandwiched eastward current is restricted to the upper 500 m layer. It seems that it is the weak bifurcation of the above recirculation when it flows northward (Fig. 6a). This argument is more explicit in Fig. 7 and would be discussed below.

Further west in the section along 144°E, the most distinct evolution is that the signal of TL is fading away. This is shown in

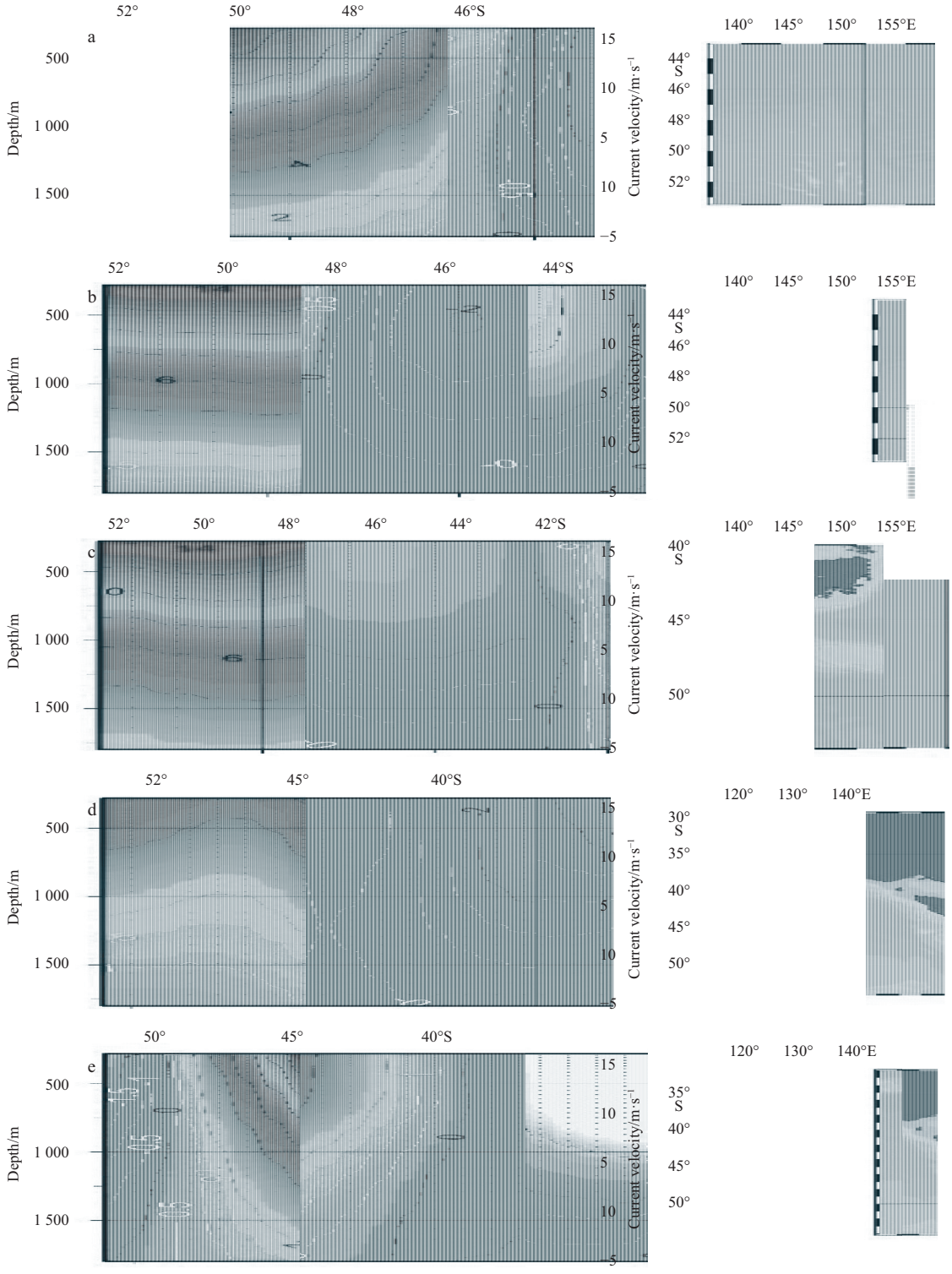

Fig. 6. Zonal current velocity (shadings, as well the east component of the geostrophic velocity) through the sequential sections to the south of Australia with the positive values representing the eastward flowing. Contour interval is 2 cm/s (0.5 cm/s) for velocity magnitude larger (less) than 2 cm/s. Along 146°E (a), 145.6°E (b), 144°E (c), 135°E (d), and 116°E (e). The corresponding section positions are shown in the maps of the right column, respectively.

Fig. 6c that the maximum speed amplitude north of 46°S is less than 3 cm/s, with no direction change. Comparing with the section at 146°E where the Tasmania extends south of 43°S into the ocean, the topography restriction here is released. As a result, the TL broadens and forms a more uniform two-core structure of current. For the sandwiched eastward current, it entirely vanishes in the 144°E section where is about 157 km away from the SR3/146°E section.

In addition to the two-core structure current south of 40°S (Fig. 6d, section along 135°E), there is a relatively weak but still

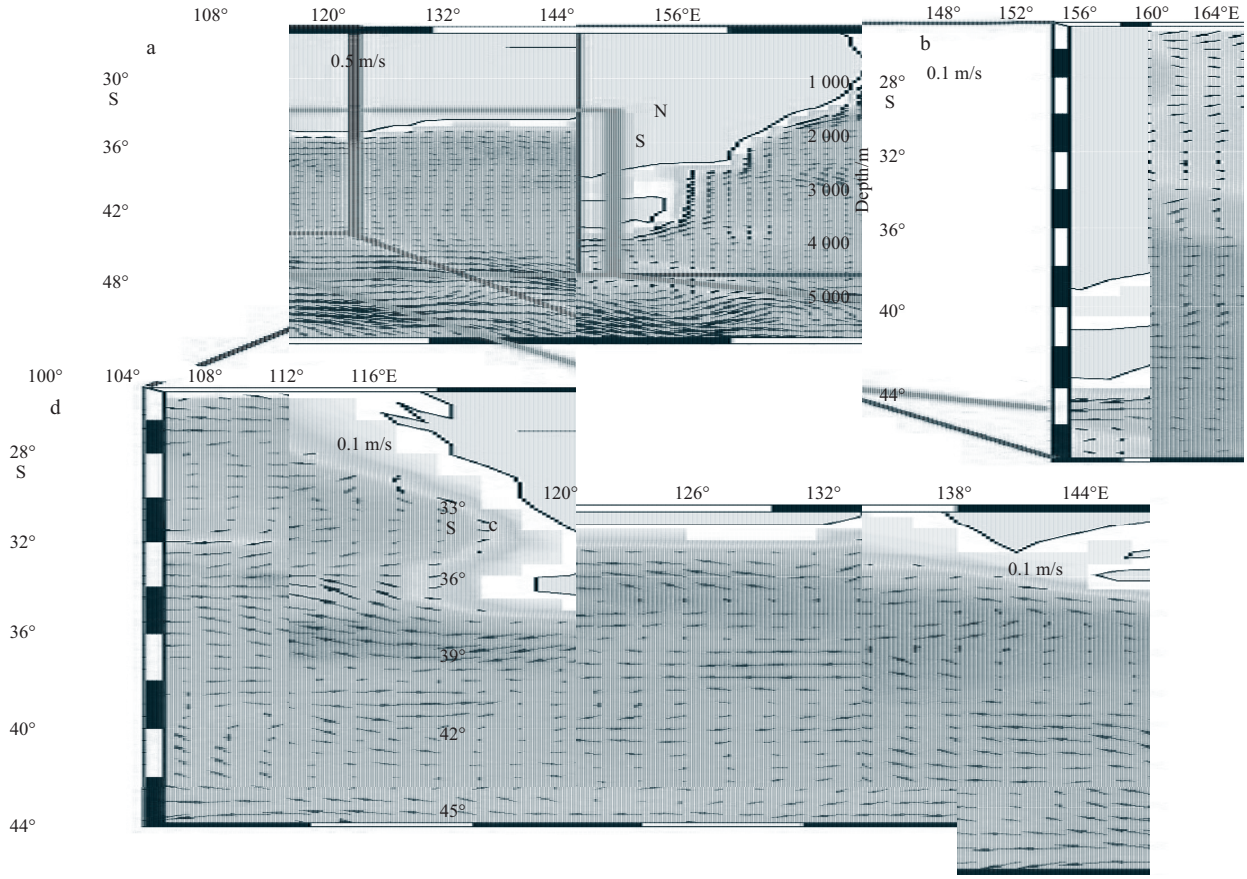

Fig. 7. The climatological field of the current velocity of AAIW (at 1 000 m water depth) for (1/2)°×(1/2)° bins (vectors) constructed from the YoMaHa'07 data, using Argo floats trajectories, with bathymetry denoting by color shadings (a). The magnification of the velocity field southeast (b), south (c) and southwest (d) to Australia are represented by red, green and blue boxes in Fig. 7a, respectively. N and S marked in the Tasman Sea represent two eddies with relatively permanent features. Note that velocity scales of Fig. 7a is different from those of Figs 7b–d.

visible westward flow near the coast, which is the Flinders Current (FC). FC is an undercurrent along the Australia's southern shelves (Middleton and Cirano, 2002). Its core centers at 600 m isobaths, is located near the slope where the westward speed can reach about 20 cm/s (Middleton and Bye, 2007). The climatological geostrophic velocity in Fig. 6d is generally consistent with the previous description of FC, though it differs from the latter a little in details. First, the westward FC north of 40°S (Fig. 6d) is strongest on the sea surface (upper layer not shown), decreasing towards the intermediate water depth; second, the overlying surface current, the Leeuwin Current (LC), is located south of the FC instead of the right above it. Nonetheless, the circulation of intermediate water is quite in agreement with the current field at 1 000 m water depth (Fig. 7).

In the westernmost section (Fig. 6e), the FC would reach its maximum speed amplitude (Cresswell and Peterson, 1993). This characteristic is apparently shown in Fig. 6e, with the speed of westward FC again being larger than 4 cm/s (1 000 m water depth), just south of the coast. Another variation is that, due to the northward migration of SAF, the westward flow in the South Australia Basin is squeezed into north of 44°S at 116°E. This at least decreases by 5° latitude width of the westward current.

6 Circulation of AAIW around South Australia

Using the data of YoMaHa'07 (Lebedev et al., 2007), a climatological field of the AAIW circulation at 1 000 m water depth (Fig. 7) is constructed. The data uncertainties of such velocity field are discussed by other works (Park et al., 2005; Katsumata and Yoshinari, 2010; Bostock et al., 2013). In addition, the climatological field of the dynamic topography (Fig. 8) at 1 000 m referenced to 2 000 m, calculated from the WOA temperature and salinity profiles are also shown for some comparison.

6.1 *AAIW circulation southeast of Australia*

AAIW circulation southeast of Australia is consisted of the EAC, a westward inflow into the South Coral Sea at approximately 28°S, a system of two anticyclonic eddies that is relatively permanent rather than transient (Sokolov and Rintoul, 2000), and an elongated anticyclonic recirculation in the south Tasman Sea.

In the intermediate water layer, the EAC is the extension of the South Equatorial Current (SEC), which enters into the Coral Sea at around 18°S (not shown here) (Sokolov and Rintoul, 2000; Ridgway and Dunn, 2003). The EAC is a strong alongshore current (Fig. 7b), flowing southward as far as the west Tasman Sea and eventually turning west across the SR3 section. During its propagation, the EAC decelerates between 35°S and 36°S, consistent with the weakening of the gradient of gravitational potential (GP) (Fig. 8).

As described above (Section 3.1), at approximately 28°S, there is a water mass truncation leading to a sharp salinity reduction in the salinity minimum, which is also suggested by Sokolov and

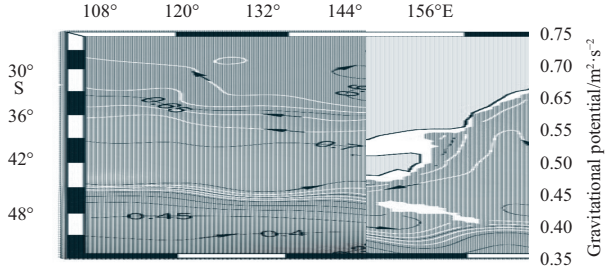

Fig. 8. Map of the climatological dynamic topography as gravitational potential at 1 000 m referenced to 2 000 m (shadings) constructed from the WOA temperature and salinity profiles. The interval of the black contours is 0.05 m^2/s^2, and 0.02 m^2/s^2 for white contours between 0.62 and 0.68 m^2/s^2. Only the black contours are labeled. The arrows represent the flowing direction of geostrophic velocity field.

Rintoul (2000). A broad westward flow from east into the south Coral Sea can be seen clearly (Fig. 7b), with its extreme southern edge locating at approximately 28°S. When this westward current encounters the EAC, they merge together and then continue flowing southward along the eastern Australian coast.

For the system of the two anticyclonic eddies at 1 000 m water depth, Eddy N (denoted in Fig. 7a) centers at around 33°S, 154°E. A branch of AAIW exports offshore at around 34°S. It turns north then west with a recirculating axis at 32°S to form an anticyclonic eddy. Within the area of this eddy the properties of water mass is quite uniform (Fig. 3d) due to mixing process. This recirculation observed from the Argo trajectories, is displayed by the 0.7 contour line in the dynamic topography (Fig. 8) as well. Eddy N's eastward flowing limb agrees with the results of previous work (Ridgway and Dunn, 2003; Ganachaud et al., 2014), but lies a little further south than that measured by Sokolov and Rintoul (2000).

The eastward limb of Eddy N is part of the TF which is measured on the sea surface (Ridgway and Dunn, 2003). But unfortunately, at least at 1 000 m depth, the TF is not evident to be a continuous eastward flow with meanders transporting through the Tasman Sea. As suggested by Mulhearn (1987) and Stanton and Ridgway (1988), the TF is influenced by the variability and instability of the EAC. And Ridgway and Dunn (2003) further proposed that the ocean topography is dominantly responsible at least for its mean flow. Thereby the vanishment of the eastward signal of TF at the intermediate water depth is seeming likely due to the blocking of Lord Howe Rise, which rises to above 1 000 m depth on the path that the TF flows (Ganachaud et al., 2014; Hu et al., 2015).

Eddy S is a warm-core anticyclonic eddy centering at 36°S, 152°E (Fig. 7b), but it is not obvious in the dynamic topography map with weak seaward GP gradient (Fig. 8). This eddy was also described by Sokolov and Rintoul (2000), though in their conclusion it is further north centered at 34°S and with larger diameter.

About the elongated anticyclonic recirculation in the south Tasman Sea, its northward inflow of AAIW from the SO enters the Tasman Sea across 43°S at about 155°E, in agreement with the hydrographic result of Sokolov and Rintoul (2000). Then the elongated northward circulation turns west and merges with the EAC south of 38°S, along the eastern coast of Tasmania. During the propagation of this recirculation, it introduces the characteristics of water mass in the SO into the Tasman Sea, and it finally spreads into the South Australia Basin.

The STF is also considered to be a barrier of water mass in this region (Hamilton, 2006; Hu et al., 2015). However, it is not obviously observed in the intermediate water layer. This is also indicated by Stanton and Ridgway (1988) and Stramma et al. (1995), that the STF is just a weak meandering to the east and a surface intensified current.

6.2 *AAIW circulation south of Australia*

South of Australia, the most significant current is the TL or TO, which is evidenced by a strong westward flow along the southern coast of Tasmania north of 46°S, as the extension of EAC (Figs 7c and 8). The data from 6-month deployment of current meters showed that a westward flow at approximately 900 m exists in the region off the west Tasmania shelf. This flow has a mean magnitude of about 4 cm/s (Middleton and Bye, 2007), which is consistent with our climatologic result here (Figs 6a and b). The TL has already been observed by previous studies (i.e., Ridgway and Dunn, 2007), and has subsequently recognized as the third route of the global Atlantic meridional overturning circulation. It connects the Pacific and Indian Oceans within the intermediate water layers (Speich et al., 2002; Speich et al., 2007).

Further west in the South Australia Basin, the AAIW has relatively uniform hydrographic properties (Fig. 3e) and apparently small current velocity (Fig. 7c), comparing with the current east of Australia. This is partly due to its semi-enclosed topographic feature. At the intermediate water depth, a westward flow occupies almost the whole basin, with few and weak eastward flow.

South of the Tasmania and along 144°E, the westward limb of the anticyclonic recirculation across the SR3 and the TL north of it converge, forming a broader westward flow (Figs 6c and 7c). When flowing across the South Australia Basin, the fairly uniform current at 145°E bifurcates into three branches when it arrives at 135°E (Figs 6d and 7c). The first one is located along the southern Australian coast. And the other two current cores lie south of 40°S, with the separation point occurring at 45°S.

In the west of South Australia Basin, there are two eddies with scale of approximately 100 km as shown in the pattern of intermediate current (Fig. 7c). Because the dynamic topography (Fig. 8) does not show the same mesoscale features, it is hard to state that these two eddies are permanently mounted there. But they have been illustrated on the sea surface from the climatological monthly sea level anomaly field (Fig. 3 in Ridgway and Condie (2004)).

The intensification of intermediate current along 116°E (Fig. 6e) can also be seen in Fig. 7c, that a 150 km width of westward flow south of Cape Leeuwin which is the strongest FC along the Australia's southern coast (Middleton and Bye, 2007).

6.3 *AAIW circulation off the southwest of Australia*

In the ocean southwest off Australia and along the coast, there is a poleward surface flow, the LC, which is driven by the large-scale meridional pressure gradient (Thompson, 1984; Godfrey and Ridgway, 1985; Ridgway and Condie, 2004). And right below the LC at 300 m water depth, the Leeuwin undercurrent (LU) is closely associated with Subantarctic Mode Water (SAMW), flowing in the opposite direction of the LC to the north (Fieux et al., 2005; Woo and Pattiaratchi, 2008). However, at the deeper depth (≈1 000 m), neither the northward nor the southward continuing flow is distinct in Fig. 7d along the western Australian coast.

Using four sections of the CTD measurement, Fieux et al. (2005) found that there is an eastward inflow around 29°S, transporting into the Perth Basin. Then it recirculates to the south along the eastern rim of the basin. This is revealed by a cyclonic

circulation (Fig. 7d) to some extent and the 0.6 contour centered around 31°S (Fig. 8).

Except for the FC coming from south of Cape Leeuwin and continuing westward into the Indian Ocean, the flowing of AAIW in the ocean west of Australia is relatively weak (speed less than 2 cm/s) and chaotic (Fig. 7d). The faint gradients of the GP in the dynamic topography (Fig. 8) also suggest such a "drawling" AAIW circulation in this study area.

7 Discussion and conclusions

Through the analysis of traditional θ-S diagrams and properties of the isopycnal (σ_0=27.2 kg/m^3) surface, the AAIW around the South Australia can be divided into five types as follows. Type 1 is the Tasman AAIW, which consists of the AAIW in the South Coral Sea and the North Tasman Sea. The AAIW of Type 1 is quite uniform both in the salinity minimum and along the isopycnal surface. It has characteristics of the highest salinity and the highest temperature in the study area, due to the replenishment from the SEC. Type 2, the SO AAIW, paralleling to and extending from the SAF, is the freshest and coldest AAIW discussed in the present work, because of the continuing replenishment from the newly formed AAIW. Type 3 is the transition of the Tasman (Type 1) and the SO (Type 2) AAIW. Through vertical and lateral mixing, the AAIW transforms into saltier and warmer variability from south to north. Type 4, the South Australia AAIW, is relatively uniform and long resident (Rintoul and Bullister, 1999; Fine et al., 2008) due to the semi-enclosed ocean bottom topography. Type 5, the southeast Indian AAIW, has the smallest meridional gradient of the salinity along the isopycnal surface in the South Indian Ocean (Wong, 2005). Here the Type 5 AAIW reveals the local transformation from the subantarctic (south) to subtropical (north) features of water mass.

We refined the Pacific-Indian interocean circulation of AAIW after analyzing the climatological field of intermediate current constructed from the Argo floats trajectories, accompanied by the climatological dynamic topography calculated from the WOA13 temperature and salinity data (Fig. 9). In the Southwest Pacific Ocean, the schematic of the intermediate current shows the same circulation features as previous studies (Sokolov and Rintoul, 2000; Ridgway and Dunn, 2003), including the EAC, the westward inflow at around 28°S, the system of two eddies, and the elongated anticyclonic recirculation. But the EAC does decelerate in the 35°–36°S latitude band, and the system of two eddies lies a little further south. In the South Australia Basin, an overview of the AAIW circulation is provided. Except for the known TL south of Tasmania and the recirculation across the SR3 section, the westward flow bifurcates into three branches in the middle of the basin. In the Southeast Indian Ocean, the inflow of intermediate water in the Perth Basin and the exiting current along the basin's eastern rim, obtained from the hydrographic analysis (Fieux et al., 2005), is confirmed. In addition, it should be noted that in this region the AAIW would mix with the subtropical Indian intermediate water, as shown by the θ-S diagram. However, there is no evident inflow revealed by the current field. Thus this implicit influence on the AAIW is represented by a dashed line in the schematic (Fig. 9).

The intermediate circulation has been proved to connect the Pacific and Indian Oceans (Fine, 1993; Talley, 1996; You, 1998; Rintoul and Sokolov, 2001; Wong, 2005) around the South Australia. The schematic of Fig. 9 illustrates this complete route, which consists of the SEC and the EAC in the Southwest Pacific Ocean, the TL and the FC in the South Australia Basin, and the extension of FC into the south Indian subtropical gyre.

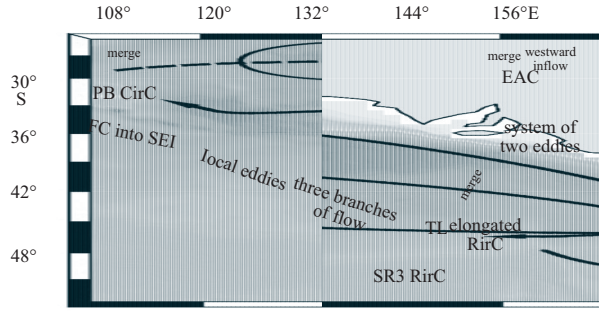

Fig. 9. The schematic of the AAIW circulation around the south Australia. RirC is the abbreviation for recirculation, CirC for circulation and PB for Perth Basin. Description about the dashed line arrow see in the text.

The Pacific-Indian interocean distribution of the AAIW has been reclassified and the circulation refined, by using the data from traditional CTD measurements and the newly developed Argo program. The present work would help to study the decadal variability of AAIW and interpret the related mechanisms.

It is worth noted that the conclusions are confined to an aspect of climatology. And it is reasonable to believe that the seasonal signal of AAIW is also of importance, as the wind field and transport stream function are quite different in the austral summer and winter (Middleton and Cirano, 2002). To achieve this goal, data of longer and better spatial coverage are necessary, including the trajectories of Argo floats and the traditional hydrographic measurements. As an essential exchange area between the Pacific Ocean and the Indian Ocean, understanding of the long-term variability of AAIW around Australia, is a vital step to study the climate change in the past, the present and the future.

Acknowledgements

The authors thank all the people who have contribute their effort to obtain the data used here.

References

Bostock H C, Sutton P J, Williams M J M, et al. 2013. Reviewing the circulation and mixing of Antarctic Intermediate Water in the South Pacific using evidence from geochemical tracers and Argo float trajectories. Deep-Sea Res: I, 73: 84–98, doi: 10.1016/j.dsr.2012.11.007

Cresswell G R, Peterson J L. 1993. The Leeuwin current south of Western Australia. Austr J Mar Freshw Res, 44(2): 285–303, doi: 10.1071/MF9930285c

Davis R E. 2005. Intermediate-depth circulation of the Indian and South Pacific Oceans measured by autonomous floats. J Phys Oceanogr, 35(5): 683–707, doi: 10.1175/JPO2702.1

Davis R E, Sherman J T, Dufour J. 2001. Profiling ALACEs and other advances in autonomous subsurface floats. J Atmos Oceanic Technol, 18(6): 982–993, doi: 10.1175/1520-0426(2001)018<0982:PAAOAI>2.0.CO;2

Donners J, Drijfhout S S. 2004. The Lagrangian view of South Atlantic interocean exchange in a global ocean model compared with inverse model results. J Phys Oceanogr, 34(5): 1019–1035, doi: 10.1175/1520-0485(2004)034<1019:TLVOSA>2.0.CO;2

Dunn J R, Ridgway K R. 2002. Mapping ocean properties in regions of complex topography. Deep-Sea Res: I, 49(3): 591–604, doi: 10.1016/S0967-0637(01)00069-3

Fieux M, Molcard R, Morrow R. 2005. Water properties and transport of the Leeuwin Current and eddies off Western Australia. Deep-Sea Res: I, 52(9): 1617–1635, doi: 10.1016/j.dsr.2005.03.013

Fine R A. 1993. Circulation of Antarctic intermediate water in the South Indian Ocean. Deep-Sea Res: I, 40(10): 2021–2042, doi:

10.1016/0967-0637(93)90043-3
Fine R A, Smethie W M Jr, Bullister J L, et al. 2008. Decadal ventilation and mixing of Indian Ocean waters. Deep-Sea Res: I, 55(1): 20–37, doi: 10.1016/j.dsr.2007.10.002
Ganachaud A, Cravatte S, Melet A, et al. 2014. The Southwest Pacific Ocean circulation and climate experiment (SPICE). J Geophys Res, 119(11): 7660–7686, doi: 10.1002/2013JC009678
Garcia H E, Locarnini R A, Boyer T P, et al. 2006. World Ocean Atlas 2005 volume 3: Dissolved Oxygen, Apparent Oxygen Utilization, and Oxygen Saturation. In: Levitus S, ed. NOAA Atlas NESDIS 63. Washington, DC: US Government Printing Office, 324
Godfrey J, Ridgway K R. 1985. The large-scale environment of the poleward-flowing Leeuwin Current, Western Australia: longshore steric height gradients, wind stresses and geostrophic flow. J Phys Oceanogr, 15(5): 481–495
Hamilton L J. 2006. Structure of the subtropical front in the Tasman Sea. Deep-Sea Res: I, 53(12): 1989–2009, doi: 10.1016/j.dsr.2006.08.013
Hu Dunxin, Wu Lixin, Cai Wenju, et al. 2015. Pacific western boundary currents and their roles in climate. Nature, 522(7556): 299–308, doi: 10.1038/nature14504
Katsumata K, Yoshinari H. 2010. Uncertainties in global mapping of Argo drift data at the parking level. J Oceanogr, 66(4): 553–569, doi: 10.1007/s10872-010-0046-4
Lebedev K V, Yoshinari H, Maximenko N A, et al. 2007. Yo Ma Ha'07: velocity data assessed from trajectories of Argo floats at parking level and at the sea surface. IPRC Technical Note, 4(2): 1–16
Mc Carthy G, Mc Donagh E, King B. 2011. Decadal variability of thermocline and intermediate waters at 24°S in the South Atlantic. J Phys Oceanogr, 41(1): 157–165, doi: 10.1175/2010JPO4467.1
Mc Carthy M C, Talley L D. 1999. Three-dimensional isoneutral potential vorticity structure in the Indian Ocean. J Geophys Res, 104(C6): 13251–13267, doi: 10.1029/1999JC900028
Middleton J F, Bye J A T. 2007. A review of the shelf-slope circulation along Australia's southern shelves: cape Leeuwin to Portland. Prog Oceanogr, 75(1): 1–41, doi: 10.1016/j.pocean.2007.07.001
Middleton J F, Cirano M. 2002. A northern boundary current along Australia's southern shelves: the flinders current. J Geophys Res, 107(C9): doi: 10.1029/2000JC000701
Molinelli E J. 1981. The Antarctic influence on Antarctic intermediate water. J Mar Res, 39(2): 267–293
Mulhearn P J. 1987. The Tasman Front: a study using satellite infrared imagery. J Phys Oceanogr, 17(8): 1148–1155, doi: 10.1175/1520-0485(1987)017<1148:TTFASU>2.0.CO;2
Orsi A H, Whitworth III T, Nowlin W D Jr. 1995. On the meridional extent and fronts of the Antarctic Circumpolar Current. Deep-Sea Res: I, 42(5): 641–673, doi: 10.1016/0967-0637(95)00021-W
Park J J, Kim K, King B A, et al. 2005. An advanced method to estimate deep currents from profiling floats. J Atmos Oceanic Technol, 22(8): 1294–1304, doi: 10.1175/JTECH1748.1
Piola A R, Georgi D T. 1982. Circumpolar properties of Antarctic Intermediate Water and Subantarctic Mode Water. Deep-Sea Res: A, 29(6): 687–711, doi: 10.1016/0198-0149(82)90002-4
Reid J L. 1989. On the total geostrophic circulation of the South Atlantic Ocean: flow patterns, tracers, and transports. Prog Oceanogr, 23(3): 149–244, doi: 10.1016/0079-6611(89)90001-3
Ridgway K R, Condie S A. 2004. The 5500-km-long boundary flow off western and southern Australia. J Geophys Res, 109(C4): doi: 10.1029/2003jc001921
Ridgway K R, Dunn J R. 2003. Mesoscale structure of the mean East Australian Current system and its relationship with topography. Prog Oceanogr, 56(2): 189–222, doi: 10.1016/S0079-6611(03)00004-1
Ridgway K R, Dunn J R. 2007. Observational evidence for a Southern Hemisphere oceanic supergyre. Geophys Res Lett, 34(13): L13612, doi: 10.1029/2007gl030392
Rintoul S R, Bullister J L. 1999. A late winter hydrographic section from Tasmania to Antarctica. Deep-Sea Res: I, 46(8): 1417–1454, doi: 10.1016/S0967-0637(99)00013-8
Rintoul S R, Sokolov S. 2001. Baroclinic transport variability of the Antarctic Circumpolar Current south of Australia (WOCE repeat section SR3). J Geophys Res, 106(C2): 2815–2832, doi: 10.1029/2000JC900107
Roemmich D, Church J, Gilson J, et al. 2015. Unabated planetary warming and its ocean structure since 2006. Nat Climate Change, 5(3): 240–245, doi: 10.1038/nclimate2513
Rosell-Fieschi M, Rintoul S R, Gourrion J, et al. 2013. Tasman Leakage of intermediate waters as inferred from Argo floats. Geophys Res Lett, 40(20): 5456–5460, doi: 10.1002/2013GL057797
Schodlok M P, Tomczak M. 1997. The circulation south of Australia derived from an inverse model. Geophys Res Lett, 24(22): 2781–2784, doi: 10.1029/97GL02576
Sloyan B M, Rintoul S R. 2001. Circulation, renewal, and modification of Antarctic mode and intermediate water. J Phys Oceanogr, 31(4): 1005–1030, doi: 10.1175/1520-0485(2001)031<1005:CRAMOA>2.0.CO;2
Sokolov S, Rintoul S. 2000. Circulation and water masses of the southwest Pacific: WOCE section P11, Papua New Guinea to Tasmania. J Mar Res, 58(2): 223–268, doi: 10.1357/002224000321511151
Speich S, Blanke B, Cai Wenju. 2007. Atlantic meridional overturning circulation and the Southern Hemisphere supergyre. Geophys Res Lett, 34(23): L23614, doi: 10.1029/2007GL031583
Speich S, Blanke B, de Vries P, et al. 2002. Tasman leakage: a new route in the global ocean conveyor belt. Geophys Res Lett, 29(10): 1416, doi: 10.1029/2001gl014586
Stanton B R, Ridgway N. 1988. An oceanographic survey of the subtropical convergence zone in the Tasman Sea. New Zealand Journal of Marine and Freshwater Research, 22(4): 583–593, doi: 10.1080/00288330.1988.9516328
Stramma L, Peterson R G, Tomczak M. 1995. The south Pacific current. J Phys Oceanogr, 25(1): 77–91, doi: 10.1175/1520-0485(1995)025<0077:TSPC>2.0.CO;2
Talley L D. 1996. Antarctic Intermediate Water in the South Atlantic. In: Wefer G, Berger W H, Siedler G, et al. The South Atlantic: Present and Past Circulation. Berlin: Springer Berlin Heidelberg, 219–238
Talley L D. 2013. Closure of the global overturning circulation through the Indian, Pacific, and Southern Oceans: schematics and transports. Oceanography, 26(1): 80–97, doi: 10.5670/oceanog.2013.07
Thompson R O R Y. 1984. Observations of the Leeuwin current off Western Australia. J Phys Oceanogr, 14(3): 623–628, doi: 10.1175/1520-0485(1984)014;0623:OOTLCO>2.0.CO;2
Tomczak M, Godfrey J S. 1994. Regional Oceanography: An Introduction. Oxford: Pergamon Press, 422
Weijer W, Sloyan B M, Maltrud M E, et al. 2012. The southern ocean and its climate in CCSM4. J Climate, 25(8): 2652–2675, doi: 10.1175/JCLI-D-11-00302.1
Wong A P S. 2005. Subantarctic mode water and Antarctic Intermediate Water in the south Indian Ocean based on profiling float data 2000–2004. J Mar Res, 63(4): 789–812, doi: 10.1357/0022240054663196
Woo M, Pattiaratchi C. 2008. Hydrography and water masses off the western Australian coast. Deep-Sea Res: I, 55(9): 1090–1104, doi: 10.1016/j.dsr.2008.05.005
Wyrtki K. 1962. The subsurface water masses in the Western South Pacific Ocean. Australian Journal of Marine and Freshwater Research, 13(1): 18–47, doi: 10.1071/MF9620018
You Y Z. 1998. Intermediate water circulation and ventilation of the Indian Ocean derived from water-mass contributions. J Mar Res, 56(5): 1029–1067, doi: 10.1357/002224098765173455